PHILIPPINE ENGINEERING JOURNAL
PEJ 2024; Vol. 45, No. 2: 39-48

Received: 15 July 2024
Received in Revised Form: 28 September 2024
Accepted: 16 November 2024

Effect of Cold-bath Quenching on Electrophoretically Deposited $Bi_2Sr_2CaCu_2O_8$ Films with Various Supporting Electrolytes

Maricar M. Rosete[1*], Myles Allen H. Zosa[2], Roland V. Sarmago[2]
[1]Department of Mining, Metallurgical, and Materials Engineering, College of Engineering, University of the Philippines Diliman, Quezon City, Philippines
[2]National Institute of Physics, University of the Philippines Diliman, Quezon City, Philippines
**Corresponding author: mmrosete@up.edu.ph*

Abstract – *Superconductors are materials that offer zero electric resistance below their transition temperature. $Bi_2Sr_2CaCu_2O_8$ (Bi-2212) is a high-temperature superconductor with many promising applications in micro-electronic devices, magnetic shielding, and high-current carrying wires. Smooth films are needed to utilize Bi-2212 for device applications. We deposited Bi-2212 films using electrophoretic deposition (EPD). The films underwent rapid thermal annealing (RTA) in air and a cold bath. All films were post-annealed. Analyses of the x-ray diffraction (XRD) and scanning electron microscopy (SEM) data reveal that cold-quenched samples maintain their crystallinity while providing a more featureless surface. However, resistance versus temperature measurements show that cold quenching degrades the superconducting properties of the films.*

Keywords: *rapid thermal annealing, electrophoretic deposition, high-temperature superconductors, supporting electrolytes, superconducting films*

I. INTRODUCTION

A superconductor is a material that has zero resistance below its superconducting transition temperature (T_c) [1]. Superconducting $Bi_2Sr_2CaCu_2O_8$ (Bi-2212) is a high-temperature superconducting material with a high T_c, chemical stability, and ease of synthesis [2, 3]. These advantages make Bi-2212 a promising candidate for micro-electronic devices, magnetic shielding, and high current-carrying wires and tapes [4, 5]. However, Bi-2212 films are required to realize the various applications of high-temperature superconductors. The films must be smooth, highly textured, and superconducting at high T_c values [3, 4, 6]. There were several efforts to produce quality Bi-2212 films. Studies have shown that quality Bi-2212 films can be achieved by melt processing followed by high cooling rates [7, 8]. Electrophoretic deposition (EPD) is a successful Bi-2212 film fabrication method [9, 10]. The process is simple, quick, and economical in preparing quality Bi-2212 films. In our previous study, we fabricated quality Bi-2212 films with optimized concentrations of different supporting electrolytes. The films had two heat treatments: rapid thermal annealing (RTA) and post-annealing. RTA creates smooth and continuous surfaces through rapid cooling. Rapid cooling impedes the nucleation of grains, resulting in the formation of even and continuous films [11]. The post-annealing step allows the re-formation of superconducting Bi-2212, safeguarding the superconducting properties of the RTA-treated films. Smooth and continuous surfaces are

essential in manufacturing superconducting devices. Hence, minimizing grain nucleation is important to realize the applications of superconductors. This study minimizes grain nucleation by quenching the films in a cold bath during RTA, which should produce a more uniform and continuous surface morphology.

II. METHODOLOGY

Bi-2212 was prepared using a conventional solid-state reaction method. The starting powders were Bi_2O_3 (99.8%), $SrCO_3$ (99.9%), $CaCO_3$ (99.9%), and CuO (99.5%) with stoichiometric amounts supplied by Sigma-Aldrich. They were thoroughly ground using an agate mortar and pestle to produce a homogenous powder mixture. The powder mixture was pressed into a pellet with a diameter of 20 mm and sintered in air at 837 ℃ for 30 hours. This procedure was repeated with intermediate grinding. The obtained sample was ground into a fine powder without further processing.

We prepared three sets of Bi-2212 suspensions using three supporting electrolytes with ethanol as the medium: 5.21 wt% KCl (Univar), 7.15 wt% NaCl (RCI Labscan), and 8.09 wt% LiCl (Riedel-de Haen), based on the optimization results from our previous study [3]. We fabricated two Bi-2212 films using EPD on Ag-coated MgO (100) substrates for each set. The EPD setup had two vertical electrodes roughly 5 mm apart and a constant applied voltage of 100 V. The substrate was on the negative electrode, and the voltage was applied for 10 minutes, depositing Bi-2212 on the substrate.

After deposition, the films underwent RTA at 970 ℃ for 10 minutes as shown in Figure 1a. Each film was loaded into a pre-heated furnace at 970 ℃. After 10 minutes, the film was either quenched in air or a cold bath. The film was removed from the furnace and exposed to ambient air for air quenching. This exposure allowed the film to rapidly cool down to room temperature. For cold quenching, the cold bath was prepared with a 1:1 ratio of ice and water to maintain a temperature of around 10 ℃. Both the ice and water were made from deionized water. After RTA, the film was submerged in the cold bath. It remained submerged for 5 minutes to ensure the film reached the temperature of the cold bath. Each film was post-annealed in a furnace at 800 ℃ for 20 hours (Figure 1b) to allow for the re-formation of superconducting Bi-2212. After annealing, the film was cooled in the furnace until it reached room temperature. All the samples were subjected to x-ray diffraction (XRD, Shimadzu Maxima 7000), field-emission scanning electron microscopy (FE-SEM, Philips XL-30), and resistance vs temperature (R-T) measurements to test the crystallinity, morphology, and superconducting properties of the films, respectively.

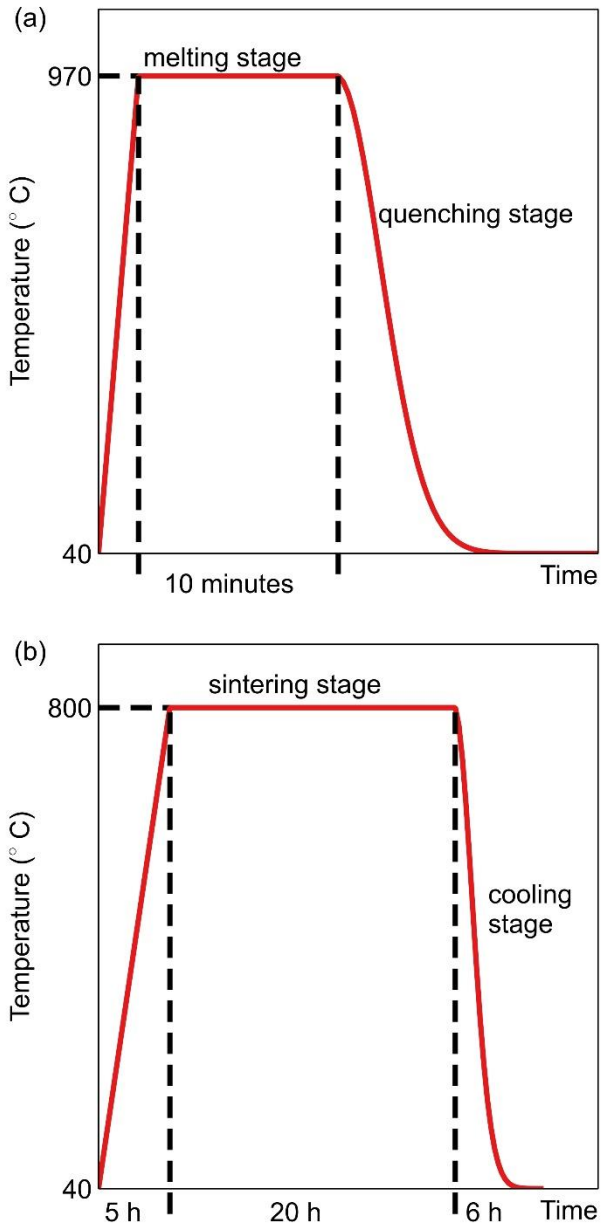

Figure 1. Temperature profiles for (a) RTA and (b) post-annealing

III. RESULTS AND DISCUSSION

According to Newton's law of cooling, rough estimations on the reduction of cooling time and the increased cooling rate a cold bath gives are given by the following equations:

$$cooling\ time\ reduction\ (\%) = \left[1 - \frac{\ln\left(\frac{T_0 - T_{cold}}{T_f - T_{cold}}\right)}{\ln\left(\frac{T_0 - T_{air}}{T_f - T_{air}}\right)}\right] \times 100\%, \quad (1)$$

$$average\ cooling\ rate\ increase\ (\%) = \left[\frac{\ln\left(\frac{T_0 - T_{air}}{T_f - T_{air}}\right)}{\ln\left(\frac{T_0 - T_{cold}}{T_f - T_{cold}}\right)} - 1\right] \times 100\%, \quad (2)$$

where T_0 is the initial film temperature, T_f is the final film temperature, T_{air} is the ambient air temperature, and T_{cold} is the cold bath temperature. Figure 2 shows that both the reduction in cooling time and increase in the average cooling rate increase with decreasing temperature. The effects of cold quenching become more apparent as time passes. Therefore, lowering the environment's temperature results in a more rapid cooling rate. Increasing the cooling rate is beneficial when the nucleation of crystals needs to be mitigated, especially during RTA. RTA aims to produce a smooth surface by partially melting and rapidly cooling the film, arresting grain growth and preventing the film from growing in patches. Thus, submerging the film in a cold bath improves the film surface quality by further mitigating crystal nucleation.

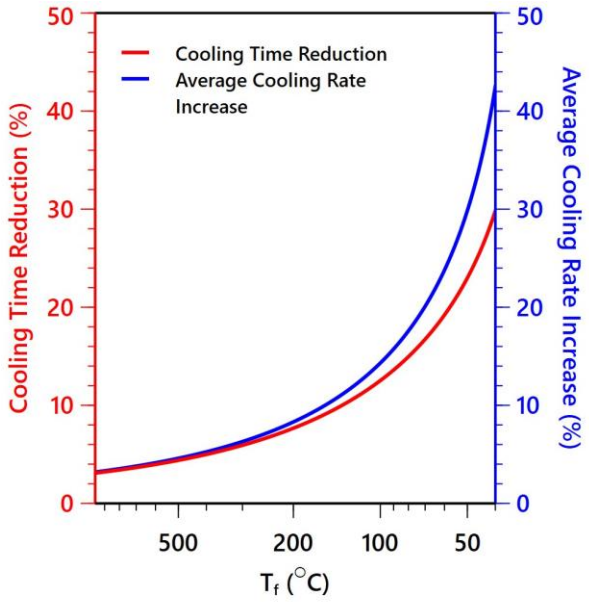

Figure 2. The cooling time reduction (red) and the cooling rate increase (blue)

The XRD graphs in Figure 3 show that all the synthesized films are c-axis oriented. All remarkable peaks shown in Figure 3 are Bi-2212 peaks excluding the peak at ~43° belonging to the MgO substrate. The c-axis orientation confirms the suitability of MgO as a substrate for Bi-2212. Furthermore, no remarkable impurity peaks are observed in Figure 3, suggesting that Bi-2212 is the dominant phase present in the films. Thus, cold quenching has no significant negative influence on film crystallinity and orientation.

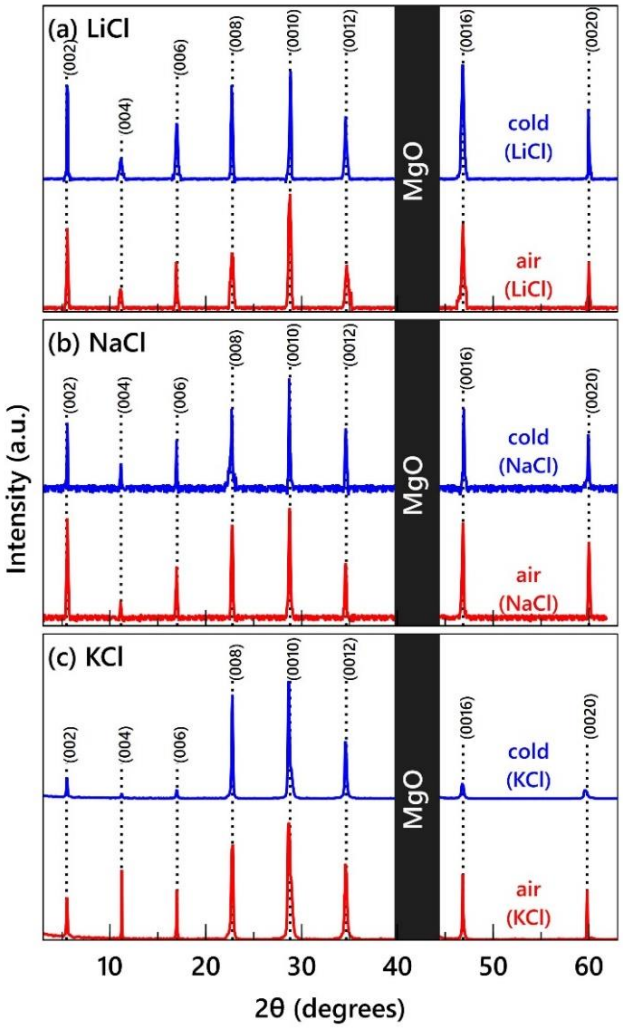

Figure 3. The XRD patterns of: (a) LiCl, (b) NaCl, and (c) KCl. The blue plots are cold-quenched, and the red plots are air-quenched

The mean crystallite size for all the films was calculated from the data in Figure 3 using the Debye-Scherrer equation,

$$D = \frac{K\lambda}{\beta \cos\theta}, \tag{3}$$

where D is the crystallite size, K is the Scherrer's constant (0.9), λ is the x-ray wavelength, β is the peak width, and θ is the Bragg angle. The crystallite sizes in Table 1 are larger when the films are cold-quenched for the LiCl and NaCl samples. The increase in crystallite size indicates that the cold-quenched samples should have fewer grain boundaries and better film coverage. On the other hand, the crystallite size is larger for the cold-quenched KCl sample. The exact reason for this trend is not clear. However, larger particle sizes are expected in KCl samples before RTA, and larger particle sizes are more resistant to melting because of their decreased surface area [3]. This could lead to sub-optimal partial melting conditions, affecting the resulting films.

Table 1. The mean crystallite size of the air and cold-quenched films.

Film	Mean Crystallite Size (nm)	
	Air Quenching	Cold Quenching
KCl	119.39	75.76
NaCl	82.44	117.86
LiCl	76.18	81.62

From the data in Figure 3, the c-lattice parameters were calculated using Bragg's law. The lattice parameters in Table 2 show no significant change in the lattice constant for LiCl and NaCl. Thus, the lattice parameter calculation for LiCl and NaCl shows no evidence of additional strain caused by cold quenching on the crystal structure. However, the lattice parameter for KCl is larger for the cold-quenched samples, indicating that cold quenching induces strain on the KCl samples.

Table 2. The calculated c lattice parameters for the air and cold-quenched samples.

Film	c Lattice Parameter (Å)	
	Air Quenching	Cold Quenching
KCl	30.89(3)	31.00(1)
NaCl	30.86(5)	30.82(4)
LiCl	30.85(5)	30.84(5)

Figures 4 and 5 show the SEM images of the air-quenched and cold-quenched Bi-2212 films. At 100x magnification in Figure 4, the films show complete substrate coverage. The average surface morphology is highlighted at 2500x magnification in Figure 5. These results show that cold-quenched films are smoother and more uniform. Unsurprisingly, the films also become smoother as the ionic radius of the cation in the supporting electrolyte decreases, which is consistent with previous results [3]. However, the air-quenched films show pronounced surface features. Although the morphological differences in the SEM images between air quenching and cold quenching are unremarkable for films fabricated using LiCl, the differences are more apparent for the NaCl and KCl films. The air-quenched NaCl and KCl films display plate-like surface growths, with the KCl film also showing cracks. In contrast,

the cold-quenched films have nearly featureless surfaces. The improved surface morphology indicates that the increased cooling rate because of the cold bath impedes nucleation to the extent that a difference in surface morphology of the fabricated films is observable.

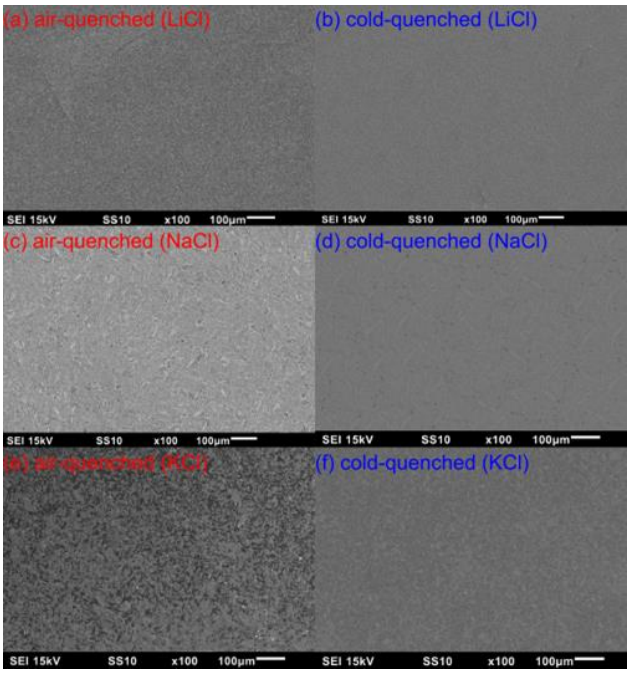

Figure 4. SEM images of the coverage air-quenched (red label) and cold-quenched (blue label) Bi-2212 films for LiCl: (a) & (b), NaCl: (c) & (d), and KCl: (e) & (f) at 100x magnification

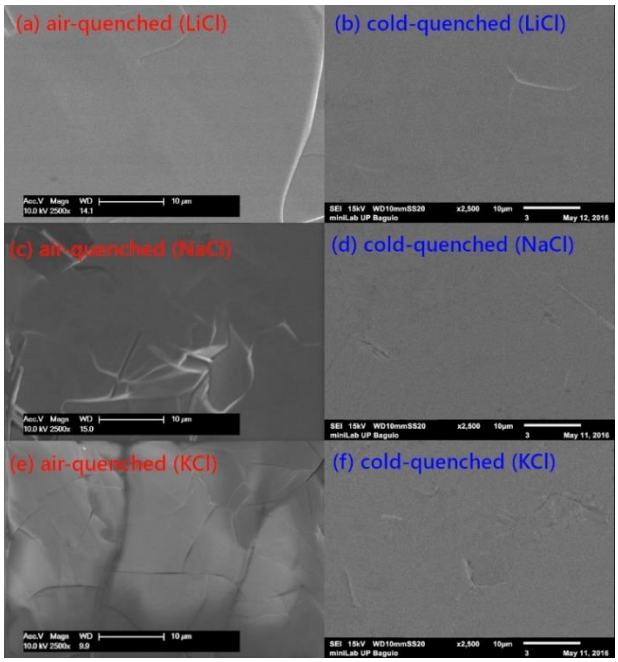

Figure 5. Surface morphology of air-quenched (red label) and cold-quenched (blue label) Bi-2212 films for LiCl: (a) & (b), NaCl: (c) & (d), and KCl: (e) & (f) at 2500x magnification

All fabricated Bi-2212 films are superconducting according to the resistance vs temperature measurements in Figure 6. In addition, every film exhibits a superconducting transition width, a characteristic of non-conventional type-II superconductors. However, the transition widths are noticeably broad for all samples. This observation suggests that there is much room to improve the annealing profile of the films to achieve narrow superconducting transitions. Additionally, there is a clear difference between the resistance vs temperature measurements for the air-quenched and cold-quenched films.

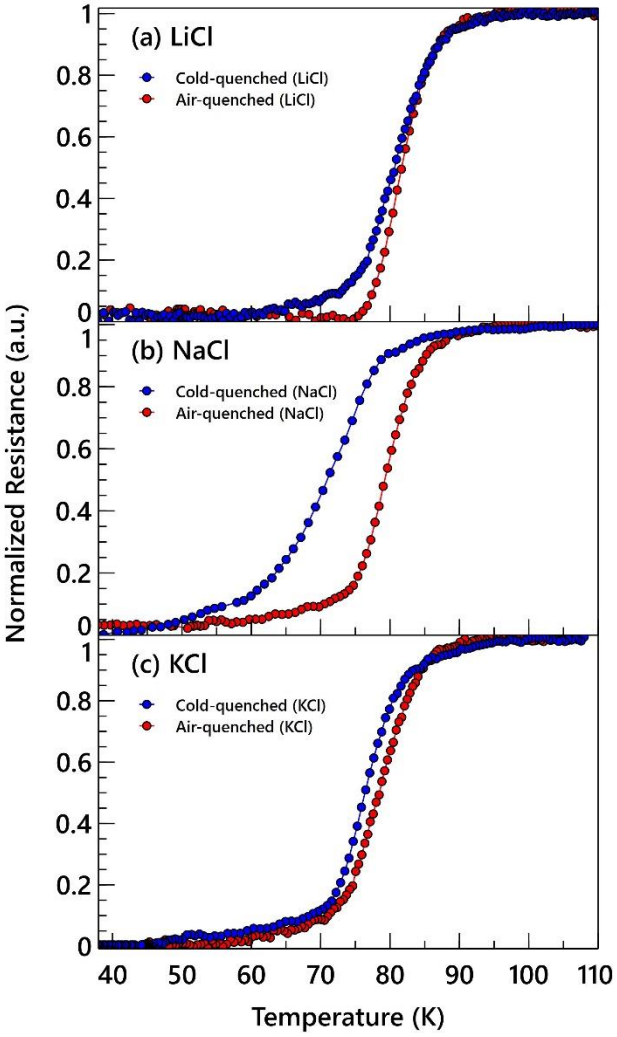

Figure 6. Resistance vs temperature measurements of cold-quenched (blue) and air-quenched (red) Bi-2212 films for: (a) LiCl, (b) NaCl, and (c) KCl

The comparison between air-quenched and cold-quenched films in Figure 7 shows that cold quenching decreases the onset superconducting transition temperature, T_c. Cold quenching also increases the superconducting transition width of the films. Consequently, cold quenching negatively affects the superconducting properties of Bi-2212 films. However, it is

possible to remedy this by optimizing the post-RTA annealing profile. The degraded superconducting properties are due to the improper reformation of Bi-2212 during the post-RTA annealing procedure. Although RTA produces smooth film surfaces, which are ideal for fabricating superconducting devices, it also destroys the superconducting properties. When a Bi-2212 film undergoes RTA, it is partially melted, dissociating its superconducting phase. Thus, the resulting film directly after RTA is not superconducting [12]. To correct this, the films undergo a post-RTA annealing procedure to reform superconducting Bi-2212. Because cold quenching further arrests the nucleation of grains, it might take more time or a higher temperature to completely reform superconducting Bi-2212 [12, 13].

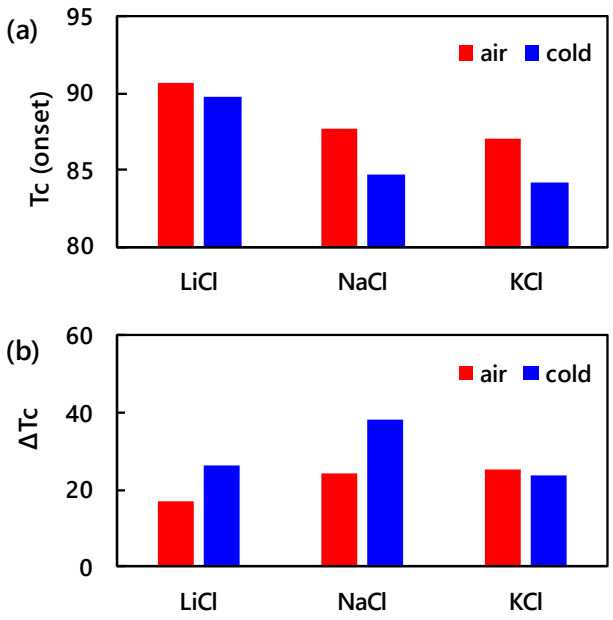

Figure 7. (a) The onset superconducting transition temperature, T_c, for air-quenched (red) and cold-quenched (blue) Bi-2212 films. (b) The superconducting transition width, ΔT_c, for air-quenched and cold-quenched Bi-2212 films

IV. SUMMARY AND CONCLUSION

We fabricated superconducting Bi-2212 films using EPD with LiCl, NaCl, and KCl as supporting electrolytes. XRD, SEM, and R-T measurements characterized crystallinity and orientation, surface morphology, and superconducting characteristics, respectively. The XRD patterns show that all films are highly c-axis oriented with no remarkable impurity peaks. Furthermore, the SEM images show that the cold-quenched films have a more featureless surface, suggesting that cold quenching further suppresses nucleation. However, the RT plots show that cold-quenching degrades the superconducting properties using the current annealing profiles.

In conclusion, cold quenching has demonstrated that it can enhance the surface morphology of EPD-grown superconducting Bi-2212 films without sacrificing their crystallinity or c-axis

orientation. These characteristics make cold-quenched films more attractive for fabricating superconducting devices. However, because cold-quenching also degrades the superconducting behavior of the Bi-2212 films, further research on the post-RTA annealing profiles is required to improve the superconducting properties of cold-quenched EPD-grown Bi-2212 films.

References:

[1] Rose-Innes AC, Rhoderick EH. 1978. Introduction to superconductivity. 2nd ed. Oxford; New York: Pergamon Press.

[2] Zhao X, Jiang L, Wang T, Liu W, Wang D, Zhang J, Zhang B, Sun B, Qi Y. 2021. A novel process for the preparation of Bi2Sr2CaCu2O8+ films with smooth surface via sol-gel method. Ceramics International. 47(17):25121-25130. doi:10.1016/j.ceramint.2021.05.242

[3] Rosete M, Zosa M, Sarmago R. 2021. Improved fabrication of electrophoretically deposited Bi2Sr2CaCu2O8 films via supporting electrolyte optimization in ethanol. Journal of Superconductivity and Novel Magnetism. 34(1):55-61. doi:10.1007/s10948-020-05668-y

[4] Shen M, Zhao G, Lei L, Ji H, Ren P. 2021. The intrinsic Josephson effect of Bi-2212 superconducting thin films prepared by sol-gel method. Ceramics International. 47(24):35067-35072. doi:10.1016/j.ceramint.2021.09.048

[5] Zhao X, Liu W, Wang T, Liu A, Li T, Chen Y, Liu X, Ma X, Sun B, Qi Y. 2021. Growth of Bi2Sr2CaCu2O8+δ thin films with enhanced superconducting properties by incorporating NiO nanoparticles. Colloids and Surfaces A: Physicochemical and Engineering Aspects. 627:127121. doi:10.1016/j.colsurfa.2021.127121

[6] Nane O, Özçelik B, Abukay D. 2013. The effects of the post-annealing temperature on the growth mechanism of Bi2Sr2Ca1Cu2O8+∂ thin films produced on MgO (100) single crystal substrates by pulsed laser deposition (PLD). Journal of Alloys and Compounds. 566:175-179. doi:10.1016/j.jallcom.2013.03.054

[7] Yang M, Goringe MJ, Grovenor CRM, Jenkins R, Jones H. 1994. The fabrication of Bi-based superconductor tape by electrophoretic deposition and melt-texturing techniques. Superconductor Science and Technology. 7(6):378-388. doi:10.1088/0953-2048/7/6/009

[8] McGinnis WC, Briggs JS. 1992. Properties of $Bi_2Sr_2CaCu_2O_8$ thick films melt-processed at temperatures up to 950 °C. Journal of Materials Research. 7(3):585-591. doi:10.1557/JMR.1992.0585

[9] Chang J-J, Jang E-S, Sohn B-H, Hwang S-J, Choy J-H. 2006. High-Tc superconducting thin film from bismuth cuprate nano-colloids. Thin Solid Films. 495(1-2):78-81. doi:10.1016/j.tsf.2005.08.304

[10] Rosete M, Zosa M, Sarmago R. 2017. Effect of potassium chloride as a supporting electrolyte on the dispersion towards the fabrication of films by electrophoretic deposition of Bi2Sr2CaCu2O8 in ethanol. Journal of Superconductivity and Novel Magnetism. 30(7):1833-1838. doi:10.1007/s10948-017-3986-8

[11] Barsoum MW. 2020. Fundamentals of ceramics. 2nd ed. Boca Raton, FL: CRC Press, Taylor & Francis Group; 2020. (Series in materials science and engineering).

[12] Aringay M, Galit E, Briones C, De Vera F, Sarmago R. 2024. Effects of varying post-annealing duration on Bi2Sr1.8In0.2CaCu2O8+δ sedimentation films. Proceedings of the 42nd Samahang Pisika ng Pilipinas. Batangas City, Philippines.

[13] Han SH, Gu GD, Shao Y, Russell GJ, Koshizuka N. 1995. The effect of annealing on the superconducting properties and structure of Bi-2212 single crystals. Physica C: Superconductivity. 246(1-2):22-28. doi:10.1016/0921-4534(95)00137-9